JJMIE

Volume 18, Number 2, June. 2024
ISSN 1995-6665
Pages 441- 453
https://doi.org/10.59038/jjmie/180216
Editor-in-Chief: Prof. Ali M. Jawarneh

Jordan Journal of Mechanical and Industrial Engineering

Springback Prediction Performance and Experimental Analysis in the V-bending Process of SCGADUB1180 Advanced High-Strength Steel

Samet Karabulut[1], İsmail Esen[2], Emrah Şahin[3*]

[1]Department of Mechanical Engineering, Faculty of Engineering, Karabük University, Karabük, Turkey
[2]Department of Mechanical Engineering, Faculty of Engineering, Karabük University, Karabük, Turkey)
[3]Department of Electricity and Energy, Vocational College, Çankırı Karatekin University, Turkey

Received 19 Dec 2023 Accepted 1 Mar 2024

Abstract

This study investigated the V-bending process of 1.2 mm thick SCGADUB1180 advanced-high-strength steel sheet plate by experimental and finite element method, and its springback behaviour was investigated in detail. In the experiments, 27 different V-bending experiments were modeled in three different punch radii (3mm, 6mm, 9mm), three different bending angle values (60°, 90° 120°), three different rolling directions (0°, 45°, 90°). In the experiments created with these input parameters, the effect of the sheets on the springback was investigated by comparing the experimental data with different material models. 108 analyses were performed for four different finite element models (Hill-48, Barlat-89, Hill-48-kinematic, Barlat-89-kinematic). It was analyzed that the Barlat-89-kinematic strain hardening model was the closest model to the experimental results. In addition, with the help of the Minitab 18.0 statistics program, how well the finite element model data agreed with the experimental results was analyzed. It was observed that the variation of punch radius (83.03%) and bending angle (8.51%) had a significant effect on the springback behaviour of the sheet. As the punch radius increased, the springback values increased. At the highest parameter level, where the bending angle was 120°, the springback values decreased. The highest springback occurred at 90° bending angle..

Keywords: Springback, Finite elements analysis (FEA), Advanced high strength steels, SCGA1180DUB, V bending, Response surface method (RSM).

1. Introduction

The automotive, aerospace and space industry responds to the needs of the sector by constantly developing new generation materials [1]. These materials have attracted attention, especially in the automotive industry, in recent years regarding impact resistance, weight, and emission reduction [2], [3]. However, these materials are difficult to form due to their high strength values [4]–[6]. Therefore, the problem of forming the improved high-strengt sheet material remains current. In addition, one of these problems is the springback of these sheet materials after the bending operation [7].

Dual-phase sheets consist of ferrite and martensite islands. Bendability is an important property for ultra-high strength sheets due to the high amount of martensite phase [8]. Being able to predict the forward or backward springing behaviour of these sheets that occur with the application of bending provides endless benefits in terms of production. If we cannot predict the springback that occurs when the punch load is removed from the sheet metal part, the die costs will increase [9]. The estimation of springback due to the bending process has attracted the attention of many researchers in recent years due to its contribution to time, money, and the environment [10]–[13].

The V-bending process is the most widely used method among sheet bending types [14]. In addition, in the literature, researchers have analyzed and discussed how the V-bending process affects high-strength sheet metal [15]–[18]. Springback, an undesirable situation, is the elastic recovery of the material, and springback needs to be measured very precisely under laboratory conditions [19]. Springback varies according to the geometry and mechanical properties of the material used [20]. Hardness, formability, lightening, and energy absorption provide great advantages for high-strength sheets [11]. However, with these advantages, high strength values increase the springback potential. Therefore, the solution to the springback problem gains importance. In recent years, many researchers have studied the springback behaviour of different sheet metal parts [21]–[26]. Studies on this subject have generally been in predicting the springback behaviour of sheet metal parts bent at different parameter levels [6], [7], [26]–[28]. All researchers also emphasized the importance of this issue. They used various finite element

* Corresponding author e-mail: emrah.sahin@karatekin.edu.tr.

models in this regard [11], [29], [30]. Finite element analysis is a technique that studies the behaviour of a part under applied forces and pressure, giving information about the states of a real object under applied loads [31][32]. With the finite element analysis, the behaviour of the part can be predicted before the part is produced, and the errors can be corrected before production [33]. Therefore, the die development process can be much more efficient with finite element or statistical estimation models, and the desired product can be obtained much faster and more accurately [34]. It is necessary to validate the prediction models with more experimental studies on this subject.

The springback of materials depends on the mechanical properties of the part and the process parameters [28]. It basically depends on parameters such as springback, yield strength, hardening exponent, anisotropy, coefficient of friction, forming speed, punch radius, bend angle, rolling directions, and material thickness [35]. The forward or backward springing of the sheet depends on the experimental design created with these parameters. Therefore, these parameters are designed to keep the forward and backward spring values to a minimum [36]. Studies show that while some parameters have a positive effect on springback, some parameters have a negative effect. For example, as the punch radius and bending angles increase, the Undesirable springback values increase [8], [35], [37], [38]. Again, another group of researchers analyzed that holding time, which reduces elastic recovery, has positive effects on springback [26], [39], [40]. They observed that sheets with good hardening properties and bends parallel to the rolling direction showed better bendability of the sheet. In addition, they analyzed that as the die angle increases, the bending moment increases, and as a result, the springbacks increase [41]. As the strength values of the sheets also increase, forming difficulties arise. Thus, as the strength of the material increases, the springback values increase. In addition, after the bending process of sheet materials is completed, the deformation and fracture behaviour should be known [23], [42]. Leu emphasized the formability properties of dual-phase sheets in her study, in which she examined the deformation behaviour of high-strength sheets. In addition, he stated that in the V-bending process, the sheets show breaking behaviour at the parts where the punch contacts the sheet at different bending angles. He commented that this situation is related to the microstructure of the sheets [35]. On the other hand, in the study in which the process parameters affecting the free bending were examined, different springback values were obtained at different speeds [27]. In addition, another study stated that 80-90% less springback occurred in samples annealed at high temperatures compared to samples annealed at low temperatures [24]. In the study, in which the effect of the V bending process and the process parameters were examined by experimental and finite element analysis, they stated that more springback was observed in the bends made perpendicular to the rolling direction compared to the tests in the rolling direction. They also emphasized the effect of the variation of the friction coefficient on the springback [43]. In summary, the increase in sheet material thickness increases the amount of springback. On the other hand, holding the punch on the sheet reduces the springback. High-strength sheets have high spring-back values due to their high strain values. On the other hand, in warm forming, the formability of the part increases with the increase in temperature, and the amount of springback is low. The general results obtained in the researches are that the decrease in the bending radius reduces the spring-back, and the increase in yield strength and hardening increases the springback [14].

The primary purpose of this study is to investigate in detail the springback behavior of SCGADUB1180 material, a high-strength sheet metal used in the automotive industry. There needs to be a study in the literature that comprehensively examines the springback properties of this special material after v-bending processes using both experimental and finite element methods. In particular, it seeks to fill a gap in the literature comparing the springback of SCGADUB1180 material with these two methods. Since the yield and tensile strength of the material are very high, defining the strain hardening exponent will be critical for the accuracy of finite element analyses. Therefore, the analysis included the strain hardening exponent for finite element models. Thus, finite element models will give results closer to reality. The study will examine the effects of material models and hardening to evaluate how effective both the original and kinematic versions of the Barlat and Hill models used in finite element analysis are in real-world conditions. Comparing these models with experimental data will reveal the strengths and weaknesses of the models and contribute to the development of models that can make more accurate predictions in the field of materials science. In addition, this study aims to create springback prediction models using regression models, and these prediction models will be compared with experimental data.

2. Materials and Methods

The material used in the study was SCGADUB1180, a new sheet material in the automotive industry. There are a limited number of studies in the literature on the springback behavior of this material. V bending The use of dual-phase steels in the automotive industry is quite common. Therefore, a 1.2 mm thick SCGA1180DUB high-strength steel sheet was chosen for the experimental research. It was subjected to tensile tests in 3 roll directions to define the material's mechanical properties in the 0°, 45° and 90° rolling directions (Figure 1b). The dimensions of the tensile test specimens are given in Figure 1a. Tensile tests were performed with MTS-100 Kn servohydraulic tester at a speed of 0.05 mm/s according to TS EN ISO 6892-1 standards (figure 1c). Tensile test specimens were prepared on a CNC laser machine (Figure 1d). After laser cutting, the samples were smoothed with a file to avoid burrs on the edges.

The engineering stress and engineering strain data obtained as a result of the tensile test were converted into true stress and true strain data using the following formulas (Eq 1, Eq 2).

$$\sigma_{true} = \sigma_{eng}(1 + \varepsilon_{eng}) \quad (1)$$

$$\varepsilon_{\text{true}} = \ln(1 + \varepsilon_{\text{eng}}) \quad (2)$$

According to the tensile test results of SCGA1180DUB high-strength steel, true stress, and true strain curves in three different rolling directions are obtained in Figure 2.

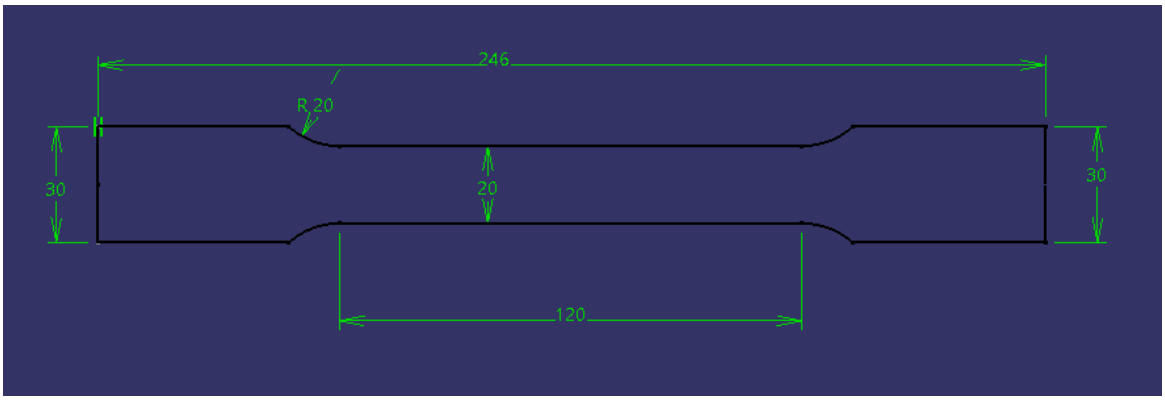

a

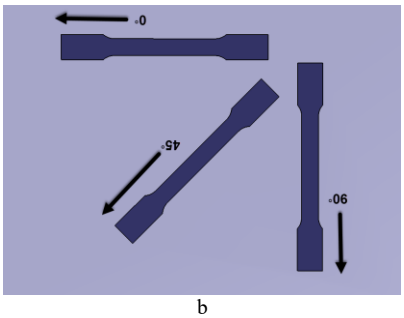

b

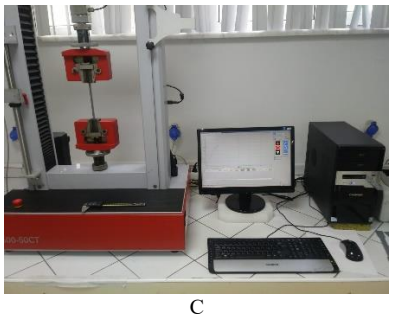

C

d

Figure 1. a. Tensile test specimen dimensions b. Tensile test specimen rolling directions c. tensile tester d. Samples after tensile test

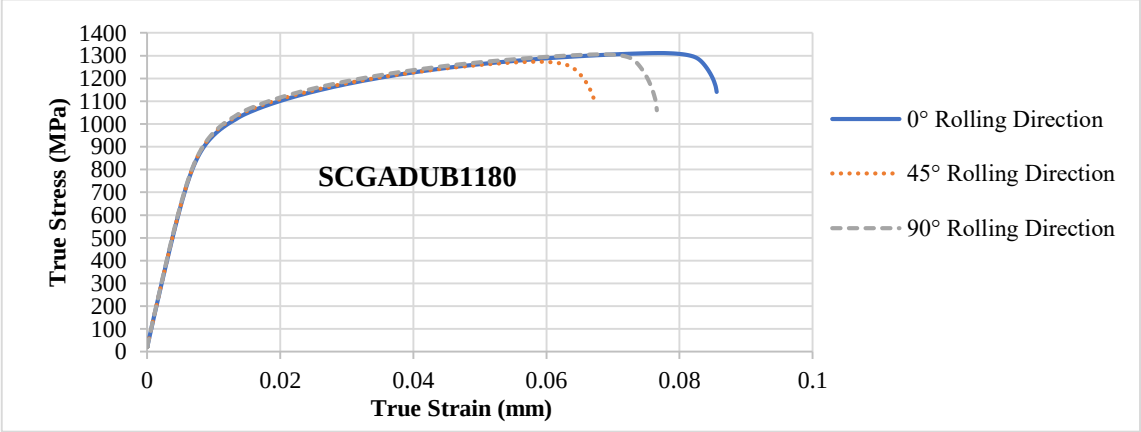

Figure 2. True stress and true strain curve of SCGADUB1180 material in three different rolling directions

According to the tensile test results, the material's mechanical properties are given in Table 1. The mechanical properties in the three different rolling directions are very close to each other. As can be seen from the graph, the amount of elongation in the 45° rolling direction is lower than in the other rolling directions.

Table 1. Mechanical properties of the material SCGADUB1180

Rolling direction	Rp0.2 (MPa)	Rm (MPa)	δ (%)	r value
0°	904.84	1217.74	6.34	0.78
45°	911.55	1202.01	4.88	0.76
90°	909.71	1221.23	5.73	0.78

The strain hardening depends on dislocation movements, forming speed, plastic forming amount, deformation direction, and temperature. In addition, repetitive loads affect plastic forming.

$$\sigma = K\varepsilon^{n} \quad (3)$$

$$\log \sigma = \log K + n \log \varepsilon \quad (4)$$

Hardening is defined as the increase in strength due to plastic deformation. Dislocations occur if the load continues with the onset of plastic deformation. It is possible to understand strain hardening in a simple way with the Holloman equations shown in Equations 3 and 4. The strain hardening exponent (n) in these equations is the ability of the material to increase strength by deformation. The K value gives information about the strength of the material. The higher the K value, the higher the strength of the material.

K (strength coefficient) and n (strain hardening coefficient) values in three different rolling directions true stress and derived from true strain curves (figure 2). Anisotropy values, the strength coefficient (K), and the

strain hardening exponent (n) specified in Table 1 and Table 2 were defined for the Hill-48 and Barlat-89 material models. Strain hardening coefficient values are close to each other in all three rolling directions.

Table 2. K and n values of the material SCGADUB1180

Rolling direction	n	K (Mpa)
0°	0.1476	1948.0
45°	0.1495	1969.6
90°	0.1505	1992.0

The samples, which were bakelite mounted for microstructure examination, were first sanded. Then the samples were then polished. The polished samples were prepared for etching by applying alcohol on their surfaces. Microstructure photographs of the materials whose surfaces were cleaned after etching were taken. In Figure 3a, the element distribution of the material SCGADUB1180 is given. As a result of the analysis, it is seen that the white islands are martensite, and the gray parts are ferrite. The chemical composition percentages of SCGADUB1180 material are presented in Table 3, and the elemental distribution is in Figure 3b.

processes were applied to this material at three different input parameter values, and the springback behaviours were simulated with both experimental and finite element models. Springback prediction models were created with finite element models. Experimental results were compared with all finite element models. In addition, the amount of interaction between ANOVA analysis and parameters was examined with the Minitab 18 statistical program. Finally, we had the chance to compare statistical and experimental data by creating a regression model [44].

2.1. Design of experiments

Test parameter levels, symbols, and values are shown in Table 4. Three different experimental parameter levels were selected for three different experimental parameters. 27 experiments were modeled according to the full factorial design. Three different die angles (60, 90, 120), three different punch radii (3, 6, 9), and three different rolling directions (0, 45, 90) were chosen as experimental parameters.

Table 3. Chemical composition of grade SCGADUB1180

Chemical composition	B	C	Al	Si	P	S	Tİ	Mn	Nb
Content (%)	13.82	50.16	0.49	2.49	0.11	0.64	2.83	29.33	0.13

Table 4. Experimental parameter values

Experimental parameter	Symbol	Units	Level		
			1	2	3
Die angle	A	degree	30	60	90
Punch radius	R	mm	3	6	9
Rolling direction	RD	degree	0	45	90

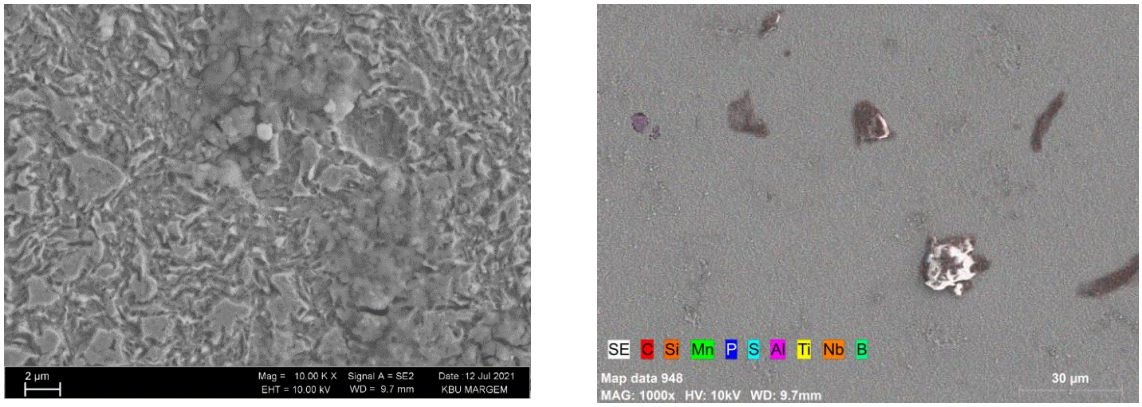

a b

Figure 3. a. Microstructure of material SCGADUB1180 b. Elemental distribution of material SCGADUB1180

a b

Figure 4. a. Connecting the die to the press with an adapter piece b. Measurement of springback in a laser optical projector.

The produced punch and matrix connected to the press are shown in Figure 4a. Axial measurements of the samples were made on the laser optical projection device (Figure 4b). Springback values were obtained by subtracting the desired size from the measurement of the samples. Figure 5a shows the shaped form of the sheet at the position where the punch applies pressure to the matrix. Figure 5b shows the amount of springback in the sheet after the punch leaves the matrix.

The shaped parts are shown in Table 5. Three bendings were made in each process. In other words, 81 experiments were conducted in total. The arithmetic average of each bending was calculated.

2.2. Finite element parameters

Finite element analyzes used in feasibility studies of sheet metal parts; The determination of material models has gained importance in the formability of parts and deformation estimations. Autoform program is widely used in finite element analysis of automobile sheets. (Figure 6) [45].

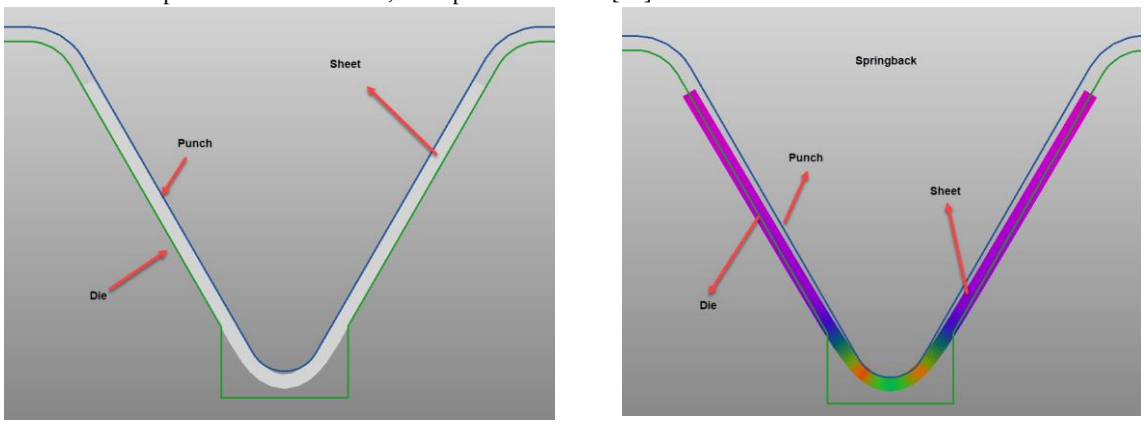

A b

Figure 5. a.Die closed state b.Display of springback after the punch leaves the sheet

Table 5. V-bend test specimens

		Punch Radius (mm)		
		R (3mm)	R (6mm)	R (9mm)
Rolling Direction (Degree)	RD (0°)			
	RD (45°)			
	RD (90°)			

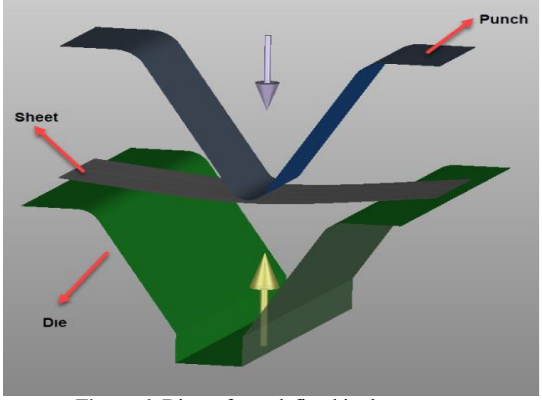

Figure 6. Die surfaces defined in the program

In the study, they were transferred to the program after the die surfaces were designed. Afterwards, the mechanical properties of the material in each rolling direction and other parameters were defined in the program (Table 1, 2, 6). For each material model, the effects of die angle (α), punch radius (R), and rolling direction (RD) on springback were investigated with the Autoform program.

Table 6. Other parameters defined in the Autoform program

Die speed	233 mm/s
Coefficient of friction	0.15
Press stroke	700 mm
Material thickness	1,2 mm

The study performed finite element analysis with four different material models. Material models of Hill-48, Barlat-89, Hill-48 + kinematic strain hardening, and Barlat-89 + kinematic strain hardening were investigated in the V bending process. Springback behaviour of SCGADUB1180 enhanced high strength steel was investigated in 4 different material models, 60°, 90°, 120° die angles, R3, R6, R9 die radii, and 0°, 45°, 90° rolling directions. 27 experiments were modeled for four different material models (Table 7). In other words, a total of 108 analyzes were made. Each analysis was transferred to the Catia environment, and the amount of springback was measured. The analysis results with these measurements were compared with the experimentally measured springback amounts.

Advanced kinematic strain hardening model in Autoform commercial software; It is defined under three main headings as early replasticization, temporary softening, and work-hardening stagnation. The hardening curve describes the hardening behavior of a material. There are alternative options for defining the stress-strain diagram. The hardening curve is found by the following formula according to the Ludwik approach. In the Ludwik formula, σ is the actual stress, K is the strength coefficient, n is the strain hardening exponent, ε is the total logarithmic strain, ε_{pl} is the plastic part of the total strain, and σ_0 is the yield stress [45].

$$\sigma = K * \varepsilon^n; \sigma(\varepsilon_{pl} = 0) = \sigma_0 \quad (5)$$

2.3. Statistical analysis

Statistical analyzes were performed with the Minitab 18.0 statistical program. With this program, it was determined how well the finite element model data were in agreement with the experimental results.

$$Y = Ø(R, \alpha, RD) \quad (6)$$

The relationship between input parameters and response parameters was investigated by Response Surface Methodology (RSM). The RSM method is widely applied in the field of engineering [46]–[48]. For example, it can be used in manufacturing to maximize efficiency, minimize the cost of a production process, or optimize the quality of a product. The response formula depending on the independent variables is presented in Equation 6. Where Y output parameter (springback); *R, α, RD* independent design variables, Ø is the response parameter function.

$$R^2 = 1 - \frac{SS_{residual}}{SS_{model} + SS_{residual}} \quad (7)$$

The R^2 determination coefficient was calculated for springback in Equation (7) SS_{model} is the sum of squares model, and $SS_{residual}$ is the sum of squares model.

The interactions between the ANOVA analysis and the parameters were obtained. Optimum parameter values were determined for optimum springback values. The regression model was created, and the regression model was compared with the experimental data.

Table 7. Experiment data and finite element models data

	INPUT PARAMETERS			OUTPUT PARAMETERS				
Experiment no.	R (mm)	α (degree)	RD (degree)	Experimental data	Barlat	Barlat kinematic	Hill	Hill kinematic
1	3	60	0	5.14	1.45	3.74	1.50	3.98
2	3	60	45	6.82	1.50	4.00	1.44	4.22
3	3	60	90	3.79	1.40	3.90	1.58	3.98
4	3	90	0	5.42	0.56	2.46	0.34	2.50
5	3	90	45	6.62	0.84	3.03	0.88	2.76
6	3	90	90	5.60	0.68	2.71	0.58	2.62
7	3	120	0	3.62	0.80	2.80	0.54	2.30
8	3	120	45	3.62	1.00	3.28	-1.00	1.60
9	3	120	90	3.10	1.64	2.76	-1.00	1.80
10	6	60	0	11.96	11.54	14.96	11.70	14.96
11	6	60	45	11.18	11.20	15.98	11.44	15.40
12	6	60	90	11.20	11.28	15.12	11.5	15.30
13	6	90	0	13.16	8.30	11.40	7.80	11.00
14	6	90	45	11.89	8.20	11.30	8.20	11.04
15	6	90	90	12.71	7.50	11.60	7.44	11.40
16	6	120	0	8.00	5.00	6.84	4.75	6.64
17	6	120	45	6.38	5.50	6.90	5.10	7.52
18	6	120	90	6.93	5.30	6.86	5.40	7.00
19	9	60	0	20.29	17.46	22.20	17.78	22.40
20	9	60	45	19.27	17.52	22.20	17.60	22.40
21	9	60	90	20.05	17.80	22.20	17.60	22.00
22	9	90	0	20.11	13.12	16.44	12.80	16.68
23	9	90	45	19.97	12.94	17.36	13.12	16.68
24	9	90	90	19.56	12.90	16.40	13.20	16.46
25	9	120	0	13.88	10.20	12.20	10.20	11.00
26	9	120	45	13.35	10.40	12.30	10.20	17.90
27	9	120	90	13.49	10.34	12.40	10.00	11.12

3. Results and Evaluation

3.1. Finite element analysis results

After the simulations were completed, the results were compared with the experimental results in terms of material models, and the accuracy of the material models in springback predictions was examined. Springback values were calculated at the last step of the analysis when the sample was released at the end of the punch stroke.

A comparative example of V-bend output for springback from the Catia program is shown in Figure 7 (for 3 mm punch radius and 60°bending angle). Detailed representations of A shown in Figure 7 are presented in Table 8. Nine different detailed images were taken from the program for die angle (α) and punch radius (R) value Each rolling direction (RD) is plotted within these nine images with different lines. In addition, four different finite element prediction models are shown in different colours.

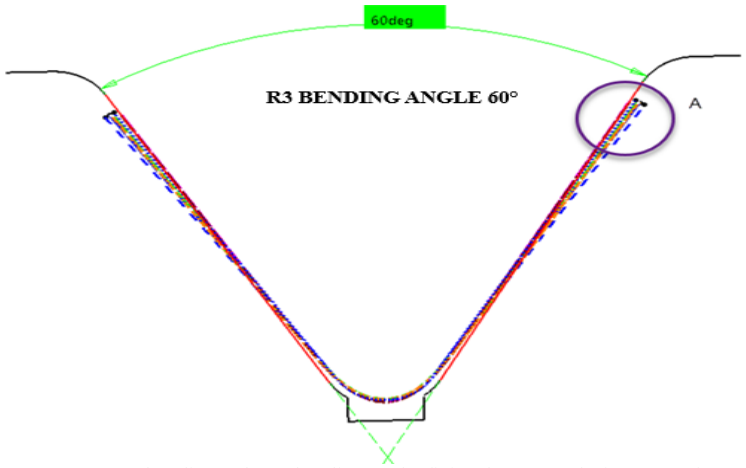

Figure 7. For 3mm punch radius and 60°, bending angle, finite element analysis outputs for springback

Table 8. Detailed finite element analysis outputs for springback

Punch Radius (mm)	Die angle (degree) 60⁰	90⁰	120⁰
3	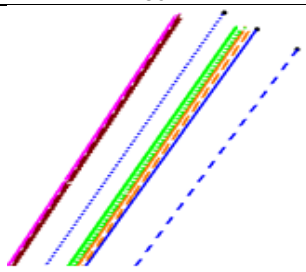	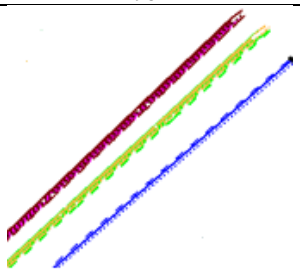	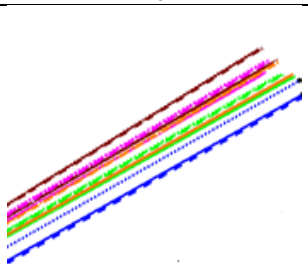
6	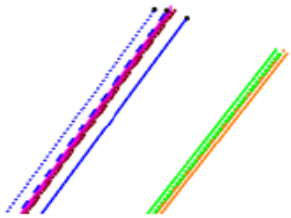	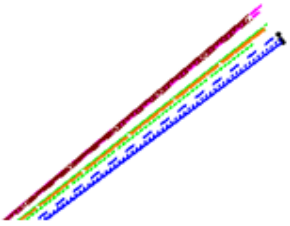	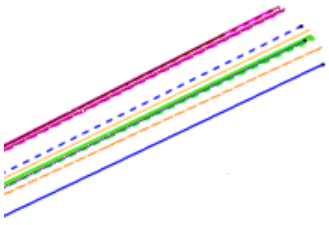
9	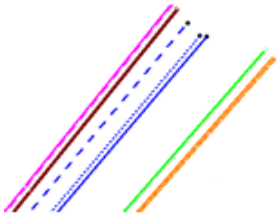	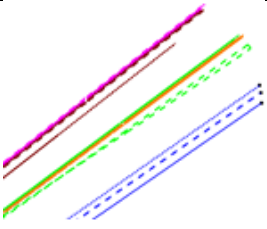	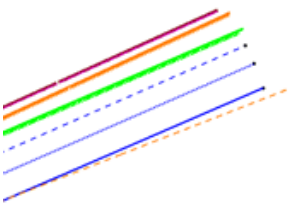

Barlat: Pink
Barlat-Kinematic Hardening: Green
Hill:Brown
Hill-Kinematic Hardening: Orange
Experemintal: Blue
0° Rolling direction:
45° Rolling direction:
90° Rolling direction:

The finite element models shown in the table are Barlat-89 (pink), Hill-48 (brown), Barlat-89 kinematic model (green), and Hill-48 kinematic model (orange). Analysis and interpretations were made according to the program outputs in the table. The best models identified with the experimental results at a 3 mm punch radius are Barlat-89 kinematic strain hardening model and Hill-48 kinematic strain hardening model. At this punch radius (R), the Barlat-89 and Hill-48 models predicted the springback values very little, according to the experimental results. Barlat-89-kinematic strain hardening and Hill-48 kinematic strain hardening models were calculated closest to the experimental springback results at 6 mm punch radius, 90°, and 120° bend angles. At the 60° bending angle, unlike the others, the Barlat-89 and Hill-48 models were calculated closest to the experimental springback results. At a 9 mm punch radius, three different rolling directions (HD) and three different bending angles (R) springbacks were obtained very close. Again, the models closest to the experimental results were the Barlat-89 kinematic strain hardening model and the Hill-48- kinematic strain hardening model.

On the other hand, the Barlat-89 kinematic strain hardening model and Hill-48 kinematic strain hardening model were not successful in predicting experimental data at a 60° bending angle, especially at 6mm and 9mm punch radii (R). Roll directions did not affect both the experimental and all finite element prediction models at the 90° bending angle; these lines are observed to overlap each other in the table. Again, as the punch radius increased at the 90° bending angle, the springback values for all rolling directions tended to move away. The best estimation of springback values was obtained at 6 mm punch radius and 90° bend angle parameter values for all finite element models.

When Figure 8 is examined, the experimental springback data and four different finite element models were compared graphically using different colours. Experimental data are shown in black. It is understood that the Barlat kinematic strain hardening finite element model, shown in orange colour, is the closest model to the experimental results. The Hill kinematic model in yellow has been analyzed to be perfect, except for the last three experiments. It is seen that the Hill and Barlat models, shown in green and blue colours, have values very close to each other. These two models have been analyzed for some experiments to have values almost identical to the experimental data. Especially in the 11th, 12th, and 13th experiments, the Hill and Barlat model and the experimental springback data are virtually identical.

3.2. Statistical analysis results

Table 9 shows the main effect plots on springback for both the experimental results and for each finite element model. It has been analyzed that the most effective parameter in terms of springback is the punch radius (R) and all models have a similar relationship with the experimental results. Afterwards, the most important parameter that was effective was the die angle (α). All models predicted that the springback decreases with increasing die angle. In reality, it was analyzed that springback increased in the transition from 60^0 die angle (α) to 90^0 die angle (α), and then the lowest values were obtained at 120^0 die angle. It has been determined according to all the results that the effect of the rolling direction (RD) for springback is not very important. It has been analyzed that the Hill-kinematic model has a different effect on the rolling direction than other finite elements and experimental results.

The ANOVA table for springback is shown in Table 10. According to this table, the most influential parameter on the springback behaviour of the sheet is the punch radius (R), with a rate of 83.03 %. Afterward, another effective parameter is the die angle (α), with a rate of 8.51%. Roll direction (RD) has no effect on springback. Again, in the ANOVA table for springback, a^2 (4.76%), R×α (1.66) and very low effect R^2 are the important interaction parameters, respectively.

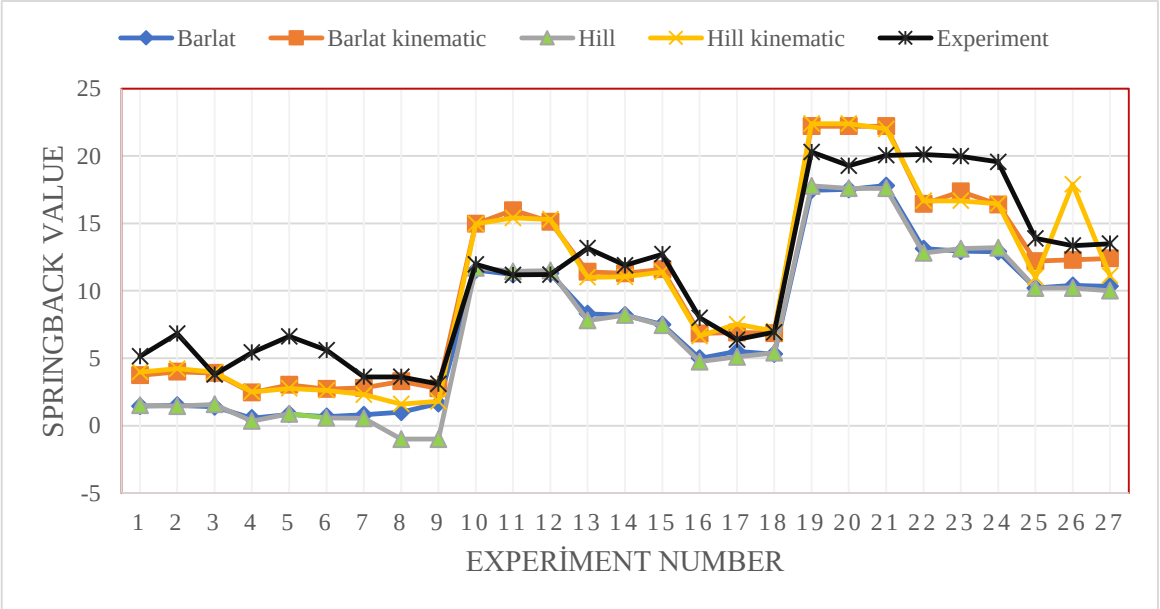

Figure 8. Comparative springback values of experimental data and finite element models

Table 9. Main effects plots for springback

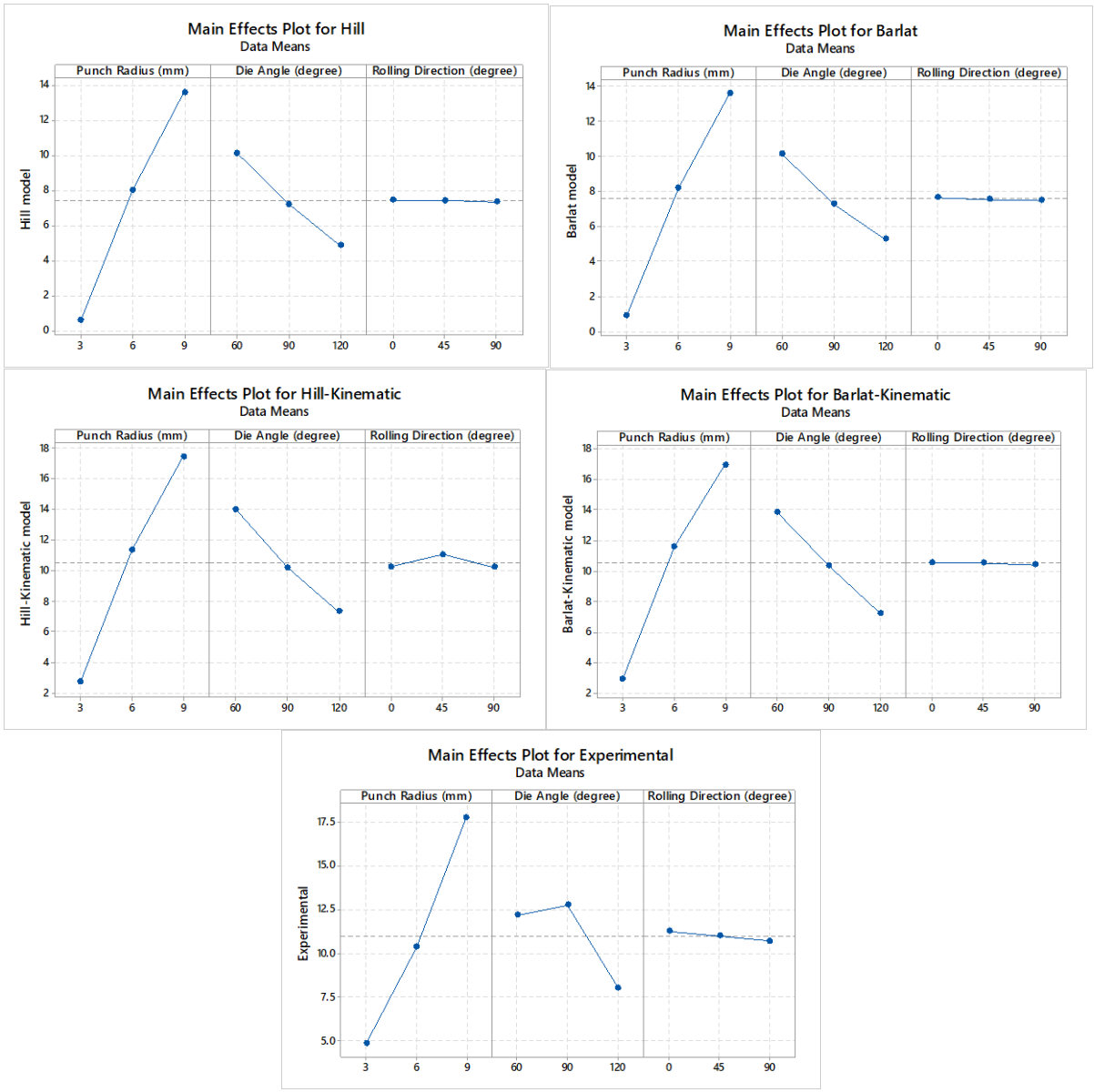

Table 10. ANOVA table for springback

Source	DF	Adj SS	Adj MS	F-Value	P-Value	Contr. %
R	1	18.018	187.018	1096.82	**≤0.001**	**83.03**
α	1	19.199	19.199	112.60	**≤0.001**	**8.52**
RD	1	0.367	0.367	2.15	0.161	0.16
R^2	1	1.300	1.300	7.63	**0.013**	**0.58**
α^2	1	10.711	10.711	62.82	**≤0.001**	**4.76**
RD^2	1	0.001	0.001	0.00	0.956	0.00
R×α	1	3.730	3.730	21.87	**≤0.001**	**1.66**
R×RD	1	0.007	0.007	0.04	0.847	0.00
α×RD	1	0.002	0.002	0.01	0.912	0.00
Error	17	2.899	0.171	-	-	1.29
Total	26	225.233	-	-	-	100.0

Significant P values are marked in bold

  - Volume 18, Number 2 (ISSN 1995-6665)

The contour plot representation for R×α, which is the most important interaction parameter according to the experimental springback results, is in Figure 9. With this contour plot, the experimental springback values increase from blue to green. It is observed that increasing the punch radius (R) increases springback. The die angle (α) value of 90^0 has the highest springback vvalue and it has been analyzed that the die angle of 120^0 keeps the springback at lower values [17].

Figure 10 shows the experimental springback values for R×α, the most important interaction parameter, with a 3D surface plot. Optimum (minimum) springback values have been obtained at the lowest punch radius (R) value (3mm) and the highest die angle (α) value (120^0).

A predictive mathematical model was constructed to understand the relationship between all experimental parameters. The necessary regression coefficient values for this model are obtained in Equation 8. The estimated springback model (Y) was constructed with the regression coefficients (β_0, $\beta_1, \beta_{2,\ldots}\beta_{33}$) calculated for each input factor (R, α, RD).

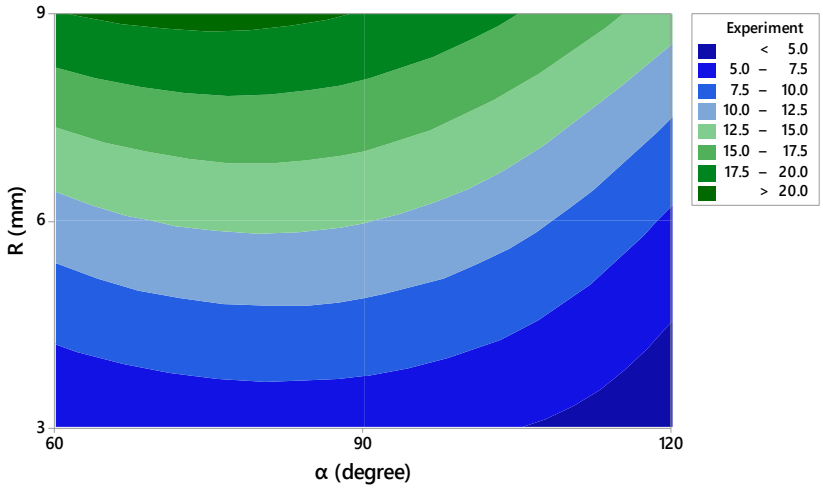

Figure 9. Contour plots for springback

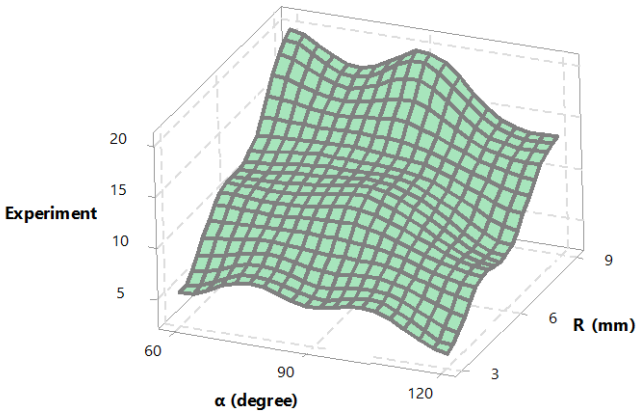

Figure 10. 3D surface plots for springback

$$\begin{aligned} Y(\text{Springback}) = \quad & \beta_0 + \beta_1 * R + \beta_2 * \alpha + \beta_3 * RD \\ & + \beta_{11} * R^2 + \beta_{22} * \alpha^2 + \beta_{33} * RD^2 \\ & + \beta_{12} * R * \alpha + \beta_{13} * R * RD + \beta_{23} * \alpha * RD \end{aligned} \quad (8)$$

The coefficients of determination and the regression formulas are presented in Equation 9.

$$\begin{aligned} \text{Experimental springback} = \quad & -21.07 + 2.011\times R + 0.5382\times\alpha - 0.0098\times RD \\ & + 0.1042\times R^2 - 0.002964\times \alpha^2 - 0.000005\times RD^2 \\ & - 0.01248\times R\times\alpha + 0.00031\times R\times RD + 0.000023\times\alpha\times RD \end{aligned} \quad (9)$$

$$\begin{aligned} R^2 &= 98.23\% \\ R^2(\text{adj}) &= 98.04\% \\ R^2(\text{pred}) &= 97.00\% \end{aligned} \quad (10)$$

The R^2 determination values calculated in Equation 10 are presented.

Experimental data on springback was compared with the estimated regression model in figure 11. Experimental data was shown in orange. The regression model is shown in blue. The prediction model and experimental data for springback were obtained very closely. The estimated R^2(pred) value of 97 % proved this situation.

4. Conclusions

In this study, V bending tests of 1.2 mm thick SCGADUB1180 enhanced high strength sheet were carried out. 27 different experiments were carried out by modeling die and material parameters (input parameters). Springback values at different bending angles (60°, 90°, 120°), different punch radii (3mm, 6mm, 9mm), and different rolling directions (0°, 45°, 90°) were investigated experimentally. In addition, the springback behaviour of this sheet was simulated with different material models (Barlat-89, Hill-48, Barlat-89 kinematic model, Hill-48 kinematic model). Furthermore, 108 analyzes were performed for 4 different finite element models. Finally, a regression model was created using statistical analysis. With this statistical program, the significance of the input parameter values of the experimental and finite element models and the relationship between the parameters were examined. Experiment results, finite element, and regression models were analyzed comparatively. The following conclusions were drawn from this study.

- SCGADUB1180 material was successfully bent in all parameters specified in the V bending process. No deformation or tear was observed in the materials. The part can be brought into the desired form with appropriate compensation values. In this study, it was analyzed that products suitable for the final geometry were obtained by using the specified parameters.
- As a result of the experimental and finite element analysis, positive springbacks were measured in almost all analyses.
- Although other finite element models agree with some experimental data, the Barlat-89 kinematic model may be more reliable in predicting springback in similar experimental setups.
- The most influential parameter on the springback behavior of the sheet was the punch radius (R), with a rate of 83.03%. Afterward, another effective parameter was the die angle (α), with a rate of 8.51%.
- Especially in process conditions with a 3 mm punch radius, springback values were low. This has been attributed to higher outer surface tension forming when low punch radii are applied to the sheet.
- Optimum (minimum) springback values were obtained with the lowest punch radius (R) value (3mm) and the highest die angle (α) value (120^0). The highest springback values were obtained at a 60° bending angle and a 9 mm punch radius.
- In addition, it was analyzed that all finite element and regression models were in a similar relationship with the experimental results. The predicted regression model for springback was obtained very close to the experimental data with a high predictive value of R^2(pred).
- According to the test results, the die angle (α) 90^0 value has the highest springback values and it has been analyzed that the 120° die angle keeps the springback at the lowest values. This situation could be attributed to the acute angle of bends, where tensile residual stresses surpass compressive stress, leading to this effect.
- As the punch radii increased, the springback values increased. At small punch radius and small bending angles, the rolling direction has a significant effect on springback. Especially in small punch radius bending process, as the bending angle increases, the effect of rolling direction on springback decreases.

Data Availability

All data generated or analyzed during this study are included in this article.

Conflicts of Interest

The authors declare no conflicts of interest.

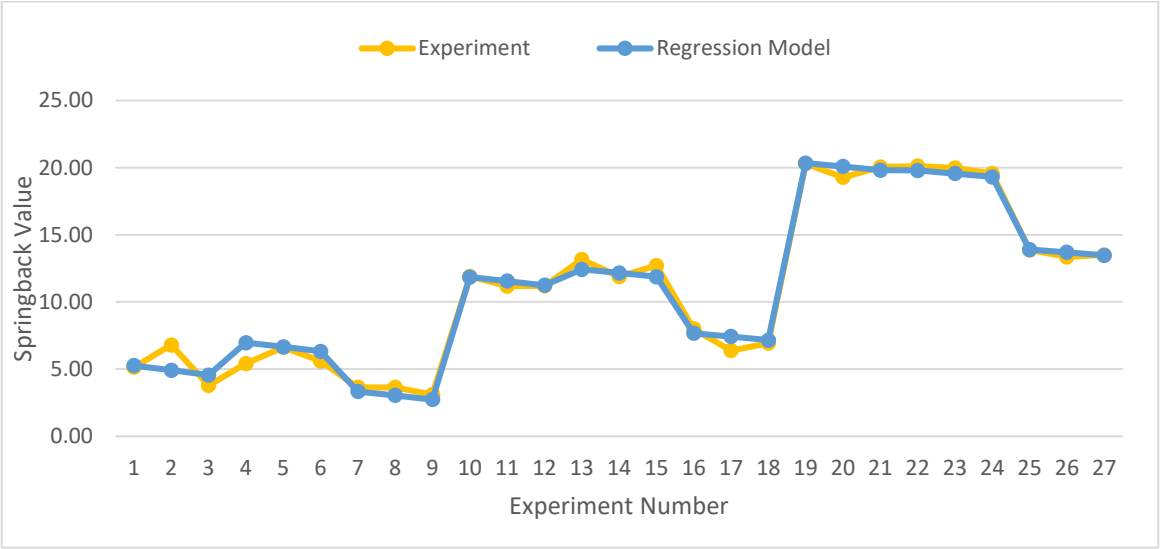

Figure 11. Comparison between predicted and measured values for springback

5. References

[1] W. Julsri and V. Uthaisangsuk, "Study of effect of varying clearances on the springback of advanced high strength steel study of effect of varying clearances on the springback of advanced high strength steel sheets," *J. Phys. Conf. Ser.*, vol. 2175, pp. 1–7, 2022, doi: 10.1088/1742-6596/2175/1/012008.

[2] M. P. Todor and I. Kiss, "Systematic approach on materials selection in the automotive industry for making vehicles lighter, safer and more fuel–efficient," *Appl. Eng. Lett.*, vol. 1, no. 4, pp. 91–97, 2016, doi: http://hdl.handle.net/10576/10425.

[3] M. Gonçalves, H. Monteiro, and M. Iten, "Life Cycle Assessment studies on lightweight materials for automotive applications - An overview," *Energy Reports*, vol. 8, pp. 338–345, Jun. 2022, doi: 10.1016/j.egyr.2022.01.067.

[4] K. Mori and Y. Abe, "A review on mechanical joining of aluminium and high strength steel sheets by plastic deformation," *Int. J. Light. Mater. Manuf.*, vol. 1, no. 1, pp. 1–11, 2018, doi: 10.1016/j.ijlmm.2018.02.002.

[5] R. Rana and S. B. Singh, *Automotive steels: design, metallurgy, processing and applications*. Woodhead, 2016. [Online]. Available: https://books.google.com.tr/books?hl=tr&lr=&id=HrszCwAAQBAJ&oi=fnd&pg=PP1&dq=The+steel+industry+responds+to+industrial+products+by+constantly+developing+new+generation+steels.&ots=GE9qxoUFuC&sig=_vnqMcj1p1xQgD-8uDaSqCwZn6g&redir_esc=y#v=onepage&q&f=false

[6] M. Wasif, M. Rababah, A. Fatima, and S. U. R. Baig, "Prediction of Springback using the Machine Learning Technique in high-tensile strength sheet metal during the V-Bending Process," *Jordan Journal of Mechanical and Industrial Engineering*, vol. 17, no. 4, pp. 481–488, 2023, doi: 10.59038/jjmie/170403.

[7] M. Rian Kurniadi *et al.*, "Preliminary study of the spring-back/spring-go phenomenon in the V-bending process using SGCC steel thin material," *J. Tek. Mesin Mech. Xplore*, vol. 3, no. 2, pp. 78–86, Dec. 2022, doi: 10.36805/jtmmx.v3i2.3370.

[8] M. Tisza and Z. Lukács, "Springback analysis of high strength dual-phase steels," *Procedia Eng.*, vol. 81, no. October, pp. 975–980, 2014, doi: 10.1016/j.proeng.2014.10.127.

[9] N. Narasimhan and M. Lovell, "Predicting springback in sheet metal forming : an explicit to implicit sequential solution procedure," *Finite Elem. Anal. Des.*, vol. 33, pp. 29–42, 1999.

[10] K. Yu, H. Choi, J. Ha, and J. Whan, "Bauschinger effect calibration by the different types of loading / reverse loading tests for springback prediction in sheet metal forming," *Int. J. Mater. Form.*, vol. 16, no. 16, pp. 1–20, 2023, doi: 10.1007/s12289-023-01738-3.

[11] Y. Hou *et al.*, "A Review of characterization and modelling approaches for sheet metal forming of lightweight metallic materials," *Materials (Basel).*, vol. 16, no. 836, pp. 1–54, 2023, doi: https://doi.org/10.3390/ma16020836.

[12] A. O. Özdemir, "Investigation of the spring-back phenomenon in two-dimensional bending of continuous glass fiber-reinforced polyamide composite sheets," *J. Compos. Mater.*, pp. 1–14, Jan. 2023, doi: 10.1177/00219983221148093.

[13] P. Mulidrán, E. Spišák, M. Tomáš, J. Majerníková, J. Bidulská, and R. Bidulský, "Impact of blank holding force and friction on Springback and its prediction of a hat-shaped part made of dual-phase steel," *Materials (Basel).*, vol. 16, no. 2, p. 811, Jan. 2023, doi: 10.3390/ma16020811.

[14] Z. Marcinak, J. L. Duncan, and S. J. Hu, *Mechanics of sheet metal forming*, Butterwort. 2002.

[15] N. Şen, T. Civek, and Ö. Seçgin, "Experimental , analytical and parametric evaluation of the springback behavior of MART1400 sheets," *J. Brazilian Soc. Mech. Sci. Eng.*, vol. 44, no. 10, pp. 1–11, 2022, doi: 10.1007/s40430-022-03749-8.

[16] S. Karabulut and İ. Esen, "Experimental investigation of the effect of process parameters on springback behavior of SCGADUB1180 high strength sheet," *Pamukkale Univ. J. Eng. Sci.*, pp. 1–10, 2022, doi: 10.5505/pajes.2022.76329.

[17] M. Wasif, S. A. Iqbal, M. Tufail, and H. Karim, "Experimental analysis and prediction of springback in V-bending process of high-tensile strength steels," *Trans. Indian Inst. Met.*, vol. 73, no. 2, pp. 285–300, Feb. 2020, doi: 10.1007/s12666-019-01843-5.

[18] M. Wasif, A. Fatima, A. Ahmed, and S. A. Iqbal, "Investigation and optimization of parameters for the reduced springback in JSC-590 sheet metals occurred during the V-bending process," *Trans. Indian Inst. Met.*, vol. 74, no. 11, pp. 2751–2760, Nov. 2021, doi: 10.1007/s12666-021-02357-9.

[19] W. . Carden, L. . Geng, D. . Matlock, and R. . Wagoner, "Measurement of springback," *Int. J. Mech. Sci.*, vol. 44, no. 1, pp. 79–101, Jan. 2002, doi: 10.1016/S0020-7403(01)00082-0.

[20] S. A. Asgari, M. Pereira, B. F. Rolfe, M. Dingle, and P. D. Hodgson, "Statistical analysis of finite element modeling in sheet metal forming and springback analysis," *J. Mater. Process. Technol.*, vol. 3, pp. 129–136, 2008, doi: 10.1016/j.jmatprotec.2007.09.073.

[21] R. Díaz, K. Nguyen, F. J. Montáns, and M. A. Sánz, "Analysis of springback of aluminum and high - strength steels through a new large strain anisotropic elastoplastic formulation based on elastic corrector rates," *Int. J. Mater. Form.*, vol. 15, no. 52, pp. 1–21, 2022, doi: 10.1007/s12289-022-01693-5.

[22] I. Ailinei, S. Galatanu, and L. Marsavina, "Influence of anisotropy on the cold bending of S600MC sheet metal," *Eng. Fail. Anal.*, vol. 137, p. 106206, 2022, doi: 10.1016/j.engfailanal.2022.106206.

[23] A. Isiktas and V. Taskin, "Springback behavior of fiber metal laminates with carbon fiber-reinforced core in V-bending process," *Arab. J. Sci. Eng.*, vol. 45, no. 11, pp. 9357–9366, Nov. 2020, doi: 10.1007/s13369-020-04796-w.

[24] S. Toros, "Parameters determination of yoshida uemori model through optimization process of cyclic tension-compression test and V-bending springback," *Lat. Am. J. Solids Struct.*, vol. 13, no. 10, pp. 1893–1911, Oct. 2016, doi: 10.1590/1679-78252916.

[25] B. I. Kazem and J. Khawwaf, "Estimation Bending Deflection in an Ionic Polymer Metal Composite (IPMC) Material using an Artificial Neural Network Model," *Jordan Journal of Mechanical and Industrial Engineering*, vol. 10, no. 2, pp. 123–131, 2016, [Online]. Available: https://pure.uniten.edu.my /en/publications/drag-reduction-in-a-wing-model-using-a-bird-feather-like-winglet

[26] M. Asmael, O. T. Fubara, and T. Nasir, "Prediction of Springback Behavior of Vee Bending Process of AA5052 Aluminum Alloy Sheets Using Machine Learning," *Jordan Journal of Mechanical and Industrial Engineering*, vol. 17, no. 1, pp. 1–14, 2023, doi: 10.59038/jjmie/170101.

[27] M. Krinninger, D. Opritescu, R. Golle, and W. Volk, "Experimental investigation of the influence of punch velocity on the springback behavior and the flat length in free bending," *Procedia CIRP*, vol. 41, pp. 1066–1071, 2016, doi: 10.1016/j.procir.2015.12.137.

[28] S. Thipprakmas and W. Phanitwong, "Process parameter design of spring-back and spring-go in V-bending process using Taguchi technique," *Mater. Des.*, vol. 32, no. 8–9, pp. 4430–4436, Sep. 2011, doi: 10.1016/j.matdes.2011.03.069.

[29] S. Bruschi *et al.*, "Testing and modelling of material behaviour and formability in sheet metal forming," *CIRP Ann. - Manuf. Technol.*, vol. 63, no. 2, pp. 727–749, 2014, doi: 10.1016/j.cirp.2014.05.005.

[30] Y. Hou, J. Min, J. Lin, Z. Liu, J. E. Carsley, and T. B. Stoughton, "Springback prediction of sheet metals using improved material models," *Procedia Eng.*, vol. 207, pp. 173–178, 2017, doi: 10.1016/j.proeng.2017.10.757.

[31] S. S. Bhavikatti, *Finite element analysis*. New Age International, 2005.

[32] M. Soori and BehroozArezoo, "Modification of CNC Machine Tool Operations and Structures Using Finite Element Methods: A Review," *Jordan Journal of Mechanical and Industrial Engineering*, vol. 17, no. 3. pp. 327–343, 2023. doi: 10.59038/jjmie/170302.

[33] H. S. S. Aljibori and A. M. Hamouda, "Finite element analysis of sheet metal forming process," *Eur. J. Sci. Res.*, vol. 33, no. 1, pp. 57–69, 2009, doi: http://hdl.handle.net/10576/10425.

[34] L. Tang, H. Wang, and G. Li, "Advanced high strength steel springback optimization by projection-based heuristic global search algorithm," *Mater. Des.*, vol. 43, pp. 426–437, Jan. 2013, doi: 10.1016/j.matdes.2012.06.045.

[35] D. K. Leu, "A simplified approach for evaluating bendability and springback in plastic bending of anisotropic sheet metals," *J. Mater. Process. Technol.*, vol. 66, no. 1–3, pp. 9–17, 1997, doi: 10.1016/S0924-0136(96)02453-3.

[36] R. Bahloul, S. Ben-Elechi, and A. Potiron, "Optimisation of springback predicted by experimental and numerical approach by using response surface methodology," *J. Mater. Process. Technol.*, vol. 173, no. 1, pp. 101–110, Mar. 2006, doi: 10.1016/j.jmatprotec.2005.11.009.

[37] D. Leu, "Position deviation and springback in V-die bending process with asymmetric dies," *Int. J. Adv. Manuf. Technol.*, vol. 79, pp. 1095–1108, 2015, doi: 10.1007/s00170-014-6532-x.

[38] Y. Chang *et al.*, "Prediction of bending springback of the medium-Mn steel considering elastic modulus attenuation," *J. Manuf. Process.*, vol. 67, no. 2, pp. 345–355, 2021, doi: 10.1016/j.jmapro.2021.04.074.

[39] Y. Zong, P. Liu, B. Guo, and D. Shan, "Springback evaluation in hot v-bending of Ti-6Al-4V alloy sheets," *Int. J. Adv. Manuf. Technol.*, vol. 76, pp. 577–585, 2015, doi: 10.1007/s00170-014-6190-z.

[40] A. Badrish, A. Morchhale, N. Kotkunde, and S. Kumar, "Parameter optimization in the thermo - mechanical V - bending process to minimize springback of Inconel 625 Alloy," *Arab. J. Sci. Eng.*, vol. 45, no. 7, pp. 5295–5309, 2020, doi: 10.1007/s13369-020-04395-9.

[41] C. Wang, G. Kinzel, and T. Altan, "Mathematical modeling of plane-strain bending of sheet and plate," *J. Mater. Process. Technol.*, vol. 39, no. 3–4, pp. 279–304, Nov. 1993, doi: 10.1016/0924-0136(93)90164-2.

[42] S. Jadhav, M. Schoiswohl, and B. Buchmayr, "Applications of finite element simulation in the development of advanced sheet metal forming processes," *BHM*, vol. 163, no. 3, pp. 109–118, 2018, doi: 10.1007/s00501-018-0713-0.

[43] T. Trzepiecinski and H. G. Lemu, "Effect of computational parameters on springback prediction by numerical simulation," *Metals (Basel).*, vol. 7, no. 9, pp. 1–14, 2017, doi: 10.3390/met7090380.

[44] U. Demircioğlu, "Classifying Cutout Shapes and Predicting Cutout Location using Regression and Classification Techniques," *Jordan Journal of Mechanical and Industrial Engineering*, vol. 17, no. 3, pp. 367–375, 2023, doi: 10.59038/jjmie/170305.

[45] M. Z. D. J. . H. S.J, *Mechanics of Sheet Metal Forming*. 2002.

[46] Sivaraos, K. R. Milkey, A. R. Samsudin, A. K. Dubey, and P. Kidd, "Comparison between taguchi method and response surface methodology (RSM) in modelling CO2 laser machining," *Jordan Journal of Mechanical and Industrial Engineering*, vol. 8, no. 1, pp. 35–42, 2014, doi: https://www.researchgate.net/profile/Mohamed-Mourad-Lafifi/post/ Can_I_optimise_a_set_of_responses_from_a_Taguchi_L9_array_using_RSM/attachment/59d64e2179197b80779a7883/AS%3A491401210273796%401494170586815/download/Comparison+between+Taguchi+Method+and+Response+Surface+Methodology+%28RSM%29+in+Modelling+CO2+Laser+Machining.pdf.

[47] C. C. Tran, V. T. Luu, V. T. Nguyen, V. T. Tran, V. T. Tran, and H. D. Vu, "Multi-objective Optimization of CNC Milling Parameters of 7075 Aluminium Alloy Using Response Surface Methodology," *Jordan Journal of Mechanical and Industrial Engineering*, vol. 17, no. 3, pp. 393–402, 2023, doi: 10.59038/jjmie/170308.

[48] E. K. Orhorhoro, E. U. Emifoniye, and S. O. Okuma, "Prediction of the Tensile Strength of an Experimental Design Reinforce Polyvinyl Chloride Composite using Response Surface Methodology," *Jordan Journal of Mechanical and Industrial Engineering*, vol. 17, no. 3, pp. 403–412, 2023, doi: 10.59038/jjmie/170309.